buildings

MDPI

Article

Protection of Structural Layers of Transitions Zones on Railways against Freezing, Using Materials with a Low Coefficient of Thermal Conductivity

Stanislav Hodas [1,*], Alzbeta Pultznerova [1] and Jana Izvoltova [2]

[1] Department of Railway Engineering and Track Management, University of Zilina, Univerzitna 8215/1, 010 26 Zilina, Slovakia; alzbeta.pultznerova@uniza.sk
[2] Department of Geodesy, University of Zilina, Univerzitna 8215/1, 010 26 Zilina, Slovakia; jana.izvoltova@uniza.sk
* Correspondence: stanislav.hodas@uniza.sk; Tel.: +421-41-513-5847

Abstract: Structural elements of railway buildings in transition zones are important parts of railway lines, where the structure of their materials is fundamentally changing. In the presented research results, these are changes in the railway body between a railway with a classic trackbed and a railway with a fixed track. The used materials of the transition zone and associated railway sections must be resistant to the effects of frost in winter. The experiments show the detected freezing depths using a zero isotherm at 0 °C. The temperature period before the onset of frost in winter is also an important factor. Numerical models of transition zones were loaded by freezing conditions. Based on the results of the experiments, frost protection measures have been proposed. To improve the temperature transition through the layers, materials with a low coefficient of thermal conductivity of transition zones have been proposed in the experimental models.

Keywords: railway buildings; transition zones; depths of freezing; layer protection; 3D numerical modeling; climatic conditions; structural materials; low coefficient of thermal conductivity

check for updates

Citation: Hodas, S.; Pultznerova, A.; Izvoltova, J. Protection of Structural Layers of Transitions Zones on Railways against Freezing, Using Materials with a Low Coefficient of Thermal Conductivity. *Buildings* **2022**, *12*, 821. https://doi.org/10.3390/buildings12060821

Received: 23 May 2022
Accepted: 11 June 2022
Published: 13 June 2022

Publisher's Note: MDPI stays neutral with regard to jurisdictional claims in published maps and institutional affiliations.

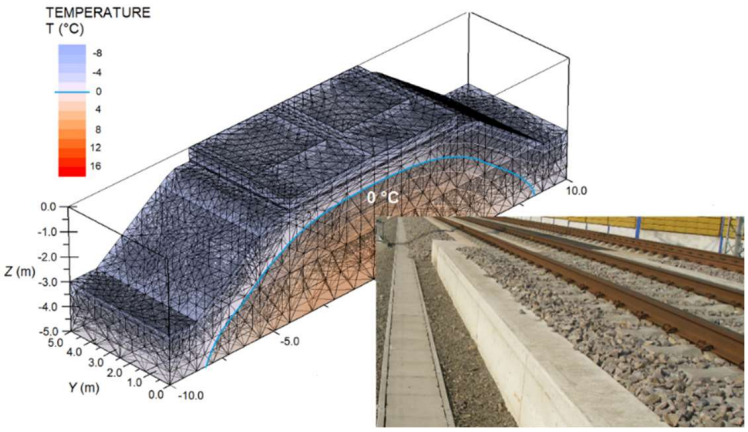
Copyright: © 2022 by the authors. Licensee MDPI, Basel, Switzerland. This article is an open access article distributed under the terms and conditions of the Creative Commons Attribution (CC BY) license (https://creativecommons.org/licenses/by/4.0/).

1. Introduction

Important elements of railway tracks are the transition zones (TZ), i.e., parts of the transition between the classic trackbed structure and the fixed track with reinforced concrete. In our case, for example, the experimental track section in Trencianske Bohuslavice near Trencin (European Railway Corridor *Va*), as shown in Figure 1a, is a numerical model, and Figure 1b shows the object that is built into the track. The research included the effects on used materials of the railway superstructure and subgrade (single-track and double-track lines, tracks on high and low embankments or cuts, and some structures of the transition zones). In the previous research activities, the effects of frost on individual railway structures were investigated by the researchers Wang and Markine [1], Dobes et al. [2], Hodas and Izvolt [3], Hodas and Pultznerova [4], Sestakova et al. [5], and Zuada Coelho and Hicks [6].

Our research started from the first day of the experiments depending on the settings of the initial temperatures, i.e., initialization in the 3D numerical modeling of the thermal regime of the transition zone. The basic question is: After which temperature period does the specific numerical modeling of the course of the temperature regime in the substructure begin? Our task is to determine the zero isotherms, i.e., line of freezing at 0 °C in the underlying structural layers. This frost disrupts the specific structures of the particular materials used in the layers of the railway substructure. Deformations of the internal structures can occur, which can be manifested by the disintegration of the shape of the object, i.e., subsequently by an undesired change in the position and height of the track geometry. The experiments also show the extent to which this observed winter season is

affected by the previous climate period. It can be a warm, medium warm, cold, or extremely cold period, etc., i.e., the required temperature initialization values are set (on the first days of the experiments). Finally, the depths of freezing of the structural elements of the transition zone are compared after the effects of previous temperature periods, which in the experiments, we label as IC1 to IC4 (as initial temperature conditions).



(**a**) (**b**)

Figure 1. Reinforced-concrete transition zones in Trencianske Bohuslavice: (**a**) numerical model [7]; (**b**) photo [Hodas]—built into track.

The most important part of the research was to determine the use of optimal materials with a low coefficient of thermal conductivity λ to protect the penetration of the frost into the lower layers of the transition zone structure. The most unfavorable winter conditions were defined at the frost index $I_F = -600$ °C·day (for a 120-day cold winter) with the initial conditions, IC4 (cold previous period). The objective of the research was to determine the optimal thicknesses of these materials (with a low coefficient of thermal conductivity $\lambda = 0.06$ to 0.12 W/m·K), which eliminates the penetration of frost to the lower layers of the transition zone.

The first part describes the object of the transition zone from the point of view of its design, built-in materials in individual parts. In this part, the frost transition without the protection of layers with elements of low coefficient of thermal conductivity is investigated. In order to present the phenomenon of deformation of the track axes in the transition zone, continuous measurements of heights in this section are shown. The second part is the verification of the frost transition in the structure using materials with a low coefficient of thermal conductivity to protect against the freezing of these materials, in particular, the layers of the structure.

All construction objects, as well as transition zones, are important for the safety of traffic for passengers and goods. Reducing maintenance costs during operation is also important from the point of view of the sustainability of the designed spatial geometric position of the railway line. Dangerous elements must be removed from the railway line. The higher the speed of the trains, the more attention needs to be paid to the buildings.

2. Transition Zone, Its 3D Numerical Model and Inspection of the Geometric Position

The transition zone on the railway track is a specific element of the structure that is built for a smooth transition and elimination of dynamic effects when there is a change in the type of railway formation (in this case, a fixed track to a track with a continuous trackbed). In railway practice, there are several building structures in these areas in different variants with different concrete thresholds (termination block) and concrete tubs with different structural arrangements (in our experiment, a double-track of the main railway corridor, track speed of $V = 160$ km/h—European Corridor *Va*).

2.1. Construction Description

In the experiments, we used the characteristic structural element of the transition zone shown in Figure 1, in which we verified the transition of temperatures to the structure of TZ (four climatic periods IC1 to IC4 before the onset of frost in the winter).

Directly at the interface of two different types of railway formations, there is a reinforced concrete threshold (other types are also proposed with a closing termination block) and a reinforced concrete tub, in which a railway ballast of variable thickness of approx. 250 to 350 mm is placed. There is also a tested elastic pad with a thickness of approx. 20 to 60 mm between gravel and reinforced concrete elements. In the top part of the transition zone structure, rails with increased resistance (for example UIC 60E3) with flexible fastening on the sleepers are proposed.

2.2. Geometry Quality Inspection of Track Axes in Object

The dynamic forces that act on the built object deform the spatial position of the track geometry. At the research facility on the track near the town of Trencin (Trencianske Bohuslavice), which is located on the European Railway Corridor *Va*, an inspection of the height behavior of the track axes has been performed using continuous measurement with a measuring trolley KRAB [8] since 2016. The transition zone is the place where the material composition of the railway body changes from a classic ballasted structure to a concrete fixed track (and vice versa), Figure 1.

The results of the long-term inspection research are presented in Figure 2a,b, where the buildings of the transition area are on both track axes of the railway line. The figures also indicate the predominant direction of travel of the train sets (approx. 90 percent).

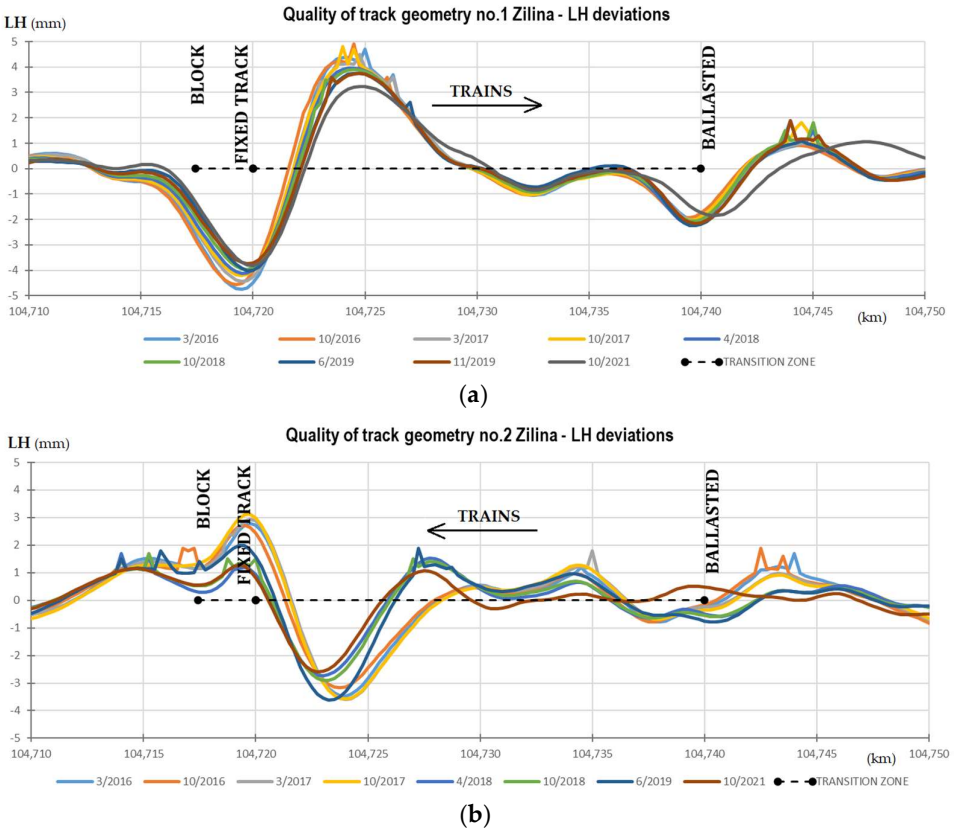


Figure 2. Inspection of track geometry quality—longitudinal height deviations (LH) of zones in Trencianske Bohuslavice from Figure 1b: (**a**) axis No. 1; (**b**) axis No. 2.

While running in front of the train, the train pushes a shock wave in the railway body, which hits an obstacle (with different stiffness of used materials), such as a fixed

track, bridge support, tunnel portal, culverts, etc. In our case, it is a concrete block of the transition zone, where the spatial position of the track axes is affected by these undesirable impact forces from railway vehicles.

2.3. Numerical Modeling of Transition Zones

Because it is a three-dimensional structural element of the transition zone on the railway line, for determination of the temperature transition (in our case, the effect of frost), it is necessary to evaluate the experiments in different directions of orientation. The SV-HEAT of SVOFFICE [7] is the most suitable solution to create a TZ model and the experimental evaluation of structural layer freezing (also used in our country for experiments for a long time). The SV-HEAT allows for these experiments and calculations, which are based on finite element calculations (formulas and calculations are part of company materials under copyright). The SV-HEAT was verified by previous research tasks and was mainly compared with the built in situ models of the heavy laboratory of the Department of Railway Engineering (DRE) by Hodas et al. [9]; Izvolt, Dobes and Hodas [10]; Izvolt, Dobes and Pies [11]; and by Sestakova and Dobes [12].

This article presents the detected changes in the depth of freezing at the onset of frost by experimental verification after various previous periods (IC1 to IC4). In individual experiments, the main winter period with a frost index of approx. $I_F = -600$ °C·day, which represents a typical cold winter in the northern part of Slovakia around the High Tatras (city of Poprad), and other cities in Europe are selected. This winter period occasionally appears in other parts of northern Slovakia (the cities of Zilina, Ruzomberok, Liptovsky Mikulas, Kosice, and others). The Poprad–Stary Smokovec–Strbske Pleso–Strba (considerable high altitude) railway line is also a specific line, but it is not the mainline of the north corridor line. This applies mainly to the northern main corridor line of the Slovak Republic through the cities of Zilina–Poprad–Kosice (European Corridor *Va*).

Material–technical characteristics of the used materials are given in the literature by Hodas and Izvol [3], SVHEAT [7], Izvolt et al. [13], Wang et al. [14], Lai et al. [15] and Navikas et al. [16,17]. These characteristics were obtained by experimental measurements in the accredited laboratories for the before-mentioned activities. Input technical characteristics of structural materials of particular layers of the railway track models in these experiments for the transition zone are considered according to Table 1 with the values of thermal conductivity λ, soil dry density ρ, specific heat capacity c, and material humidity w.

Table 1. Technical characteristics of structural layer materials.

Particular Regions of the R*i* Model (Material)	λ **(J/day·m·K)**	λ**/24.60.60 (W/m·K)**	ρ **(kg/m^3)**	c **(J/kg·K)**	w **(%)**
Railway ballast (R7, R8)	60,000	0.69	1908	980	2
Reinforced concrete (R3–R6)	136,000	1.57	2400	1020	2
Subgrade (R2, R9, R10)	130,000	1.50	2081	1585	17
Subsoil (R1)	105,000	1.22	1646	1495	18

To increase the value of the effect of frost in the experiment, we can use a cold winter with a low snow thickness of approx. 0.10 m (due to the fact that the snow is an excellent thermal insulator and the snow height is also adjusted by the train's run). The conversion constant n_F represents the sum of the temperature difference measured at the height of 2 m above the ground with the surface temperature of the transition part and the temperature reduction in terms of snow thickness. We can take into account the calculation constant $n_F = 0.75$ or determine it by measuring at the experimental in situ stands.

3. Results of Monitored Climatic Quantities of In Situ Experiments

In our university science park at outdoor in situ laboratories, day-long temperatures (24 h/per 30 min) were recorded by measurements of climatic conditions in the winter periods 2003–2022 for our Zilina region in the Slovak Republic by Dobes et al. [2], VEGA [18,19], and Izvolt et al. [10]. The monitoring was aimed at investigating the passage of these temperatures from the surface to the particular structural layers of the railway line to determine the freezing depth D_F (at 0 °C). Due to global warming of the Earth in recent decades, even on these in situ models (experimental stands), warmer winters were measured, which can be included in the periods IC1 and IC2. However, our task was to determine the depth of freezing during the coldest winters with the frost index $I_F = -600$ to -800 (°C·day) according to IC3 and IC4. The reason is to determine the thicknesses of the individual railway track structures to resist the freezing conditions.

During all measurements on in situ stands, the largest frost index $I_F = -388$ °C·day was recorded in the winter of 2005/2006, where the largest freezing depths around $D_F = -0.82$ m were also in our region, which is represented only by period IC2.

Measurements took place on two stands, at No. 1 in the years 2003–2016 and after moving to the Faculty of Civil Engineering, the measurements continued on the new stand No. 2 from 2013 until today. The measured values are presented in Tables 2 and 3.

Table 2. Overview of monitored climatic characteristics at the experimental stand No. 1 **.

Winter Period *	Maximum Mean Daily Air Temperature $\theta_{s,max}$ (°C)	Minimum Mean Daily Air Temperature $\theta_{s,min}$ (°C)	Air Frost Index I_F (°C·day)	Air Frost Index on Surface I_{FS} (°C·day)	Depth of Freezing D_F (m)
2003 * 2004	13.2	−12.3	−168	−58	0.46
2004 * 2005	8.0	−13.4	−228	−143	0.70
2005 * 2006	5.7	−16.7	−388	−248	0.82
2006 * 2007	13.0	−5.3	−16	−14	0.33
2007 * 2008	8.6	−8.2	−96	−91	0.48
2008 * 2009	11.1	−11.8	−150	−130	0.58
2009 * 2010	10.4	−13.3	−204	−149	0.60
2010 * 2011	5.7	−12.3	−215	−145	0.61
2011 * 2012	4.9	−15.2	−238	−207	0.98
2012 * 2013	10.7	−11.4	−162	−54	0.44
2013 * 2014	11.2	−10.5	−27	−33	0.46
2014 * 2015	9.1	−9.0	−40	−20	0.34
2015 * 2016	5.1	−7.6	−49	−72	0.47

** Measurements of this experimental stand were finished in 2016.

Table 3. Climatic characteristics achieved from measurements at the experimental stand No. 2 ***.

Winter Period *	Maximum Mean Daily Air Temperature $\theta_{s,max}$ (°C)	Minimum Mean Daily Air Temperature $\theta_{s,min}$ (°C)	Air Frost Index I_F (°C·day)	Air Frost Index on Surface I_{FS} (°C·day)	Depth of Freezing D_F (m)
2013 * 2014	10.4	−11.7	−38	−24	0.43
2014 * 2015	8.5	−10.8	−77	−38	0.42
2015 * 2016	5.5	−10.2	−99	−71	0.49
2016 * 2017	4.2	−19.0	−284	−248	0.65
2017 * 2018	8.1	−11.2	−107	−66	0.58
2018 * 2019	6.7	−11.3	−125	−58	0.47
2019 * 2020	10.9	−7.65	−50	−28	0.37
2020 * 2021	11.0	−12.4	−110	−27	0.36

*** Measurements of this new experimental stand started in 2013.

Due to the warm course of individual winters, the research focuses on numerical modeling of the temperature passage through the particular structural layers of the railway lines for temperature periods such as IC3 and IC4.

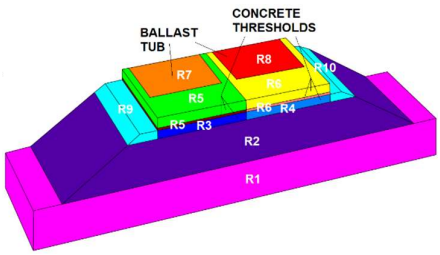
4. Experiments—Modeling with Different Climatic Pre-Periods

In the standards of some countries, there are different procedures for particular weather specifications (mild, medium, cold, extremely cold, etc.) or according to the different water regimes under the terrain at the place of the transition zone object. In the experiment, four temperature periods were determined before the main calculation of the detection of the depth of frost penetration (curve, respective 3D surface with a temperature of 0 °C penetration through the layers of the TZ structure). Simply put, as autumn was, the heat was accumulated in the landscape in layers below the surface of the terrain, including the railway structures. The designation of these experiments is IC1 to IC4 from the warmest to the coldest temperature of the previous period. It is also determined by real measurements in the layers below the surface of the terrain. In the heavy in situ laboratory of DRE, thermometers were placed at certain depths, in an amount of approx. 150–200 pcs., including moisture measurements at certain depths of the structure according to Hodas et al. [9] and Izvolt et al. [10]. The individual structural layers TZ are designated as regions R*i*, where: R1, R2, ... are the lower layers and ... R9, R10, ... are the layers upward of the TZ model of the railway track.

During the numerical modeling, the accumulated heat, which is characterized by the temperature in the particular regions of the R*i* model, is given in Table 4 (with the scheme of the R*i*). For the data, the values of these temperatures were adjusted into 4 °C intervals to determine the regularity of the behavior of the temperature transitions.

Table 4. Initial temperatures IC*i* as the initial condition (from previous periods: pre-periods).

Previous Periods Structure R*i* (Material)	IC1	IC2	IC3	IC4
		(°C)		
R1	22	18	14	10
R2	20	16	12	8
R3, R4	18	14	10	6
R5, R6	16	12	8	4
R7, R8	16	12	8	4
R9, R10	16	12	8	4



After selection, for example for autumn, according to the characteristics of IC*i* (IC1 to IC4), the final modeling of the frost transition through the "TZ" layers will follow during the winter period.

In the conclusions, the results of changes in the depths of freezing of the TZ structure are presented. In this modeling, a cold winter with $I_F = -600$ °C·day was used according to a known graph of daily temperatures during 120 days of winter (regularly used for experiments in Figure 3).

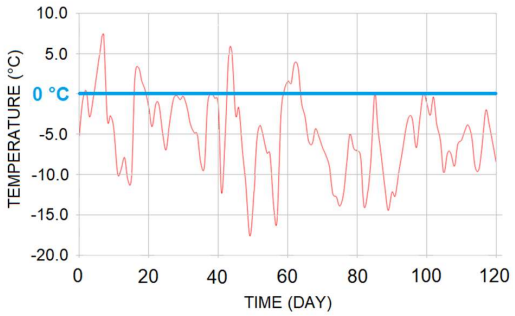


Figure 3. Graph of daily temperatures (IC3)—cold winter 120 days, $I_F = -600$ °C·day.

5. Experiment—A Numerical Model of the Transition Zone

Subsequently, after choosing the previous climatic period IC1 to IC4, the main calculation of a specific object of the transition zone with the cold winter was performed gradually according to the graph of daily temperatures in Figure 3. The advantage of 3D modeling in this experiment after model processing, including calculations, is that the different sections displaying the temperature mode can be selected using a plane in any 3D position and its rotation.

The most important cuts are the longitudinal sections in the axes of the tracks, specifically directly below the particular rails, the axes of the transition element, and cross-sections through the reinforced concrete block or the reinforced concrete tub with a ballast. A transition object is a complex 3D structure.

For example, the result of the experiment is the cross-section for Y = 4 m, where there is a reinforced concrete tub with a ballasted trackbed displayed in Figure 4 (3D view in Figure 4a, cross-section of temperature isotherms in Figure 4b and cross-section with 0 °C isotherms in Figure 4c).

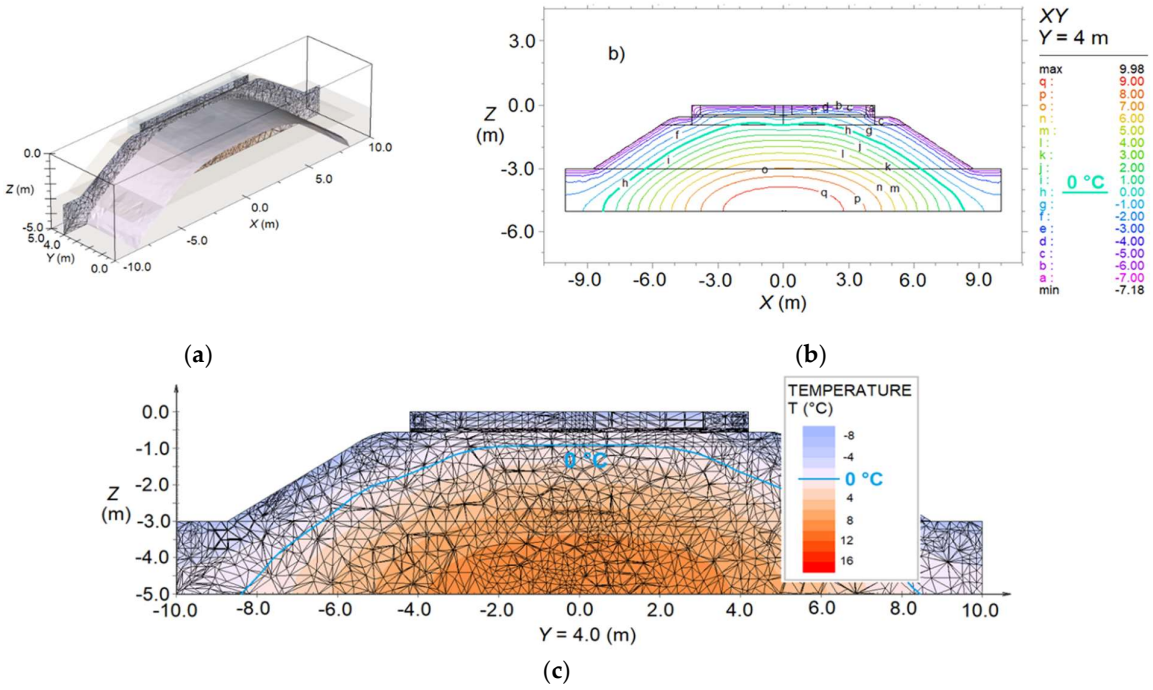


Figure 4. Graphic outputs Y = 4 m: (**a**) 3D view; (**b**) isotherms; (**c**) cross-section.

Similar sections with results can be displayed in experiments in large numbers according to their requirements; the data are also stored in data files. The section, which presents the longitudinal section $X = \pm 2.1$ m directly below the rail, is shown in Figure 5, where there is also the greatest traffic load from the wheel pressures of the trains (except for the effects of frost). The experimental outputs are given for the previous climatic period IC3, and the main calculation is for winter with $I_F = -600$ °C·day. The frost index I_F is the sum of negative temperatures measured four times per day, and the I_F period begins with the first frosts lasting for at least 4 consecutive days. In the experiments, the numerical modeling during the winter is 120 days, e.g., winter period from November to March of the following year. The TZ model was shown at a length of 5 m, as this would represent high demands on data and time. The gradient of the ballasted trackbed can be taken into account by another small model in the required cross-section of the 3D model. The total length of the construction in the transition zone for the required line speed of V = 160 km/h has a designed length of approx. 22 m.

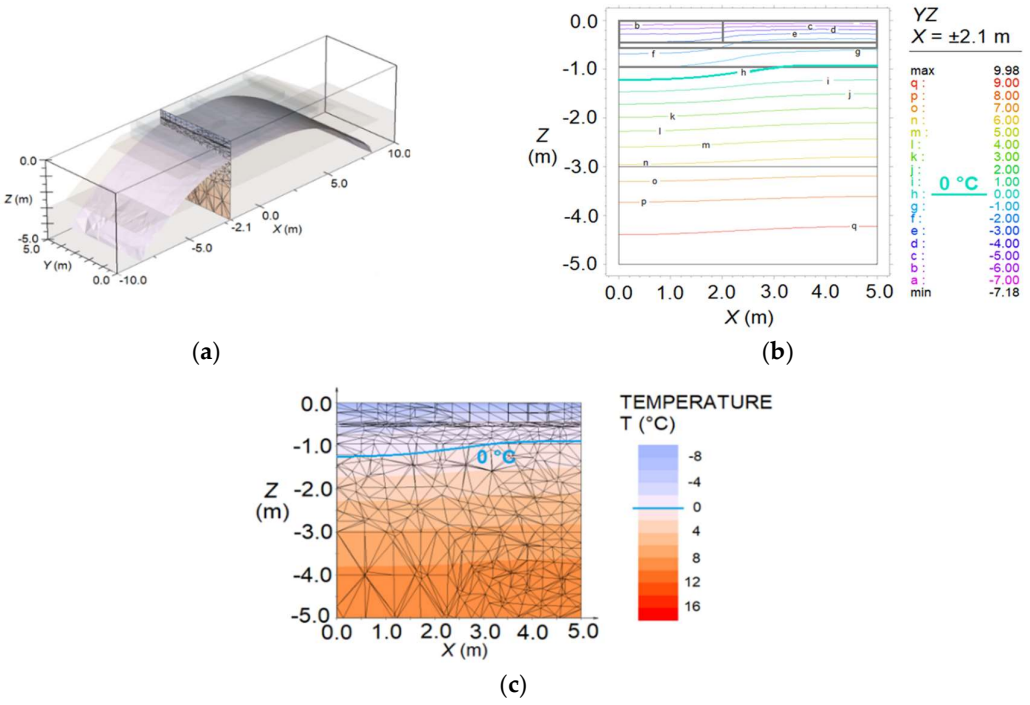


Figure 5. Graphic outputs X = 2.1 m: (**a**) 3D view; (**b**) isotherms; (**c**) cross-section.

6. Evaluation and Discussion

The results of the experiments can be assessed and analyzed from the point of view of the influence of temperature in the period before frost on the course of experiments that influences the investigated models. The resulting values are gradually loaded by the decreasing temperatures in the previous period, i.e., IC1 to IC4 according to Table 4, where the initialization temperatures on the model surface in parts R7 to R10 are from 16 °C to 4 °C. This involves heating the layers below the surface and is changing more slowly than the temperatures in the air. From a temperature point of view, the differences between these periods are large, from the warm period (16 °C) to the cold (4 °C). The typical pre-period for testing is the IC3 structure, where the outdoor temperature is 8 °C (this is before calculating the tested model), and then, we consider the onset of winter in experiments. The selection was also suitable for other experiments that have already been performed by Hodas, Izvolt and Dobes [9] and Hodas and Pultznerova [4]. Figures 6 and 7 show the final freezing depths of the layers for all IC1 to IC4 periods, based on which the analysis was performed.

In the transition part, the results are presented mainly for the following parts: reinforced concrete block (threshold) and reinforced concrete tub with a railway bed. The characteristic course of temperatures is shown by the results of longitudinal sections in 3D, where the course of freezing of the particular layers of the structure is also shown at the same time, i.e., for example, below the rail or in the track axis of a single or double track (Figure 6 for IC3 pre-period). In the case of these experiments, i.e., of the specific transition zone, the control area is the lower surface of the bottom of the reinforced concrete structure at a depth of −0.95 m at the beginning of the investigated element.

Detailed results with the analysis of freezing, i.e., the location of the zero isotherms with 0 °C, are given in Figure 7 for all temperature pre-periods of the IC1 to IC4. In Figure 6a, considerable freezing occurs for a part of the reinforced concrete block (threshold), because the reinforced concrete material is not a good thermal insulator. The depth of freezing varies, as can be seen in Figure 6b, where a ballasted trackbed with a lower value of thermal conductivity (λ) is built in. During the experiments, all values of Figure 6a,b were verified with values of Figure 6c, where the track axis in the longitudinal profile is X = 2.10 m (on position 2 of Figure 8). The positions in Figure 6 of the column values for Y = 1.00 m and Y = 4.00 m are identical with X = 2.10 m.

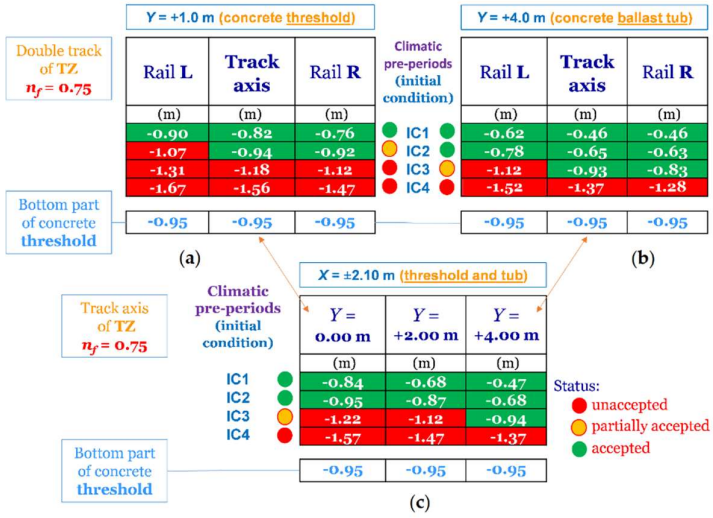


Figure 6. Results of experiments and analysis of freezing depths h: (**a**) iron-concrete threshold Y = +1.0 m; (**b**) concrete tub with ballast bed Y = +4.0 m; (**c**) threshold and tub X = ±2.10 m.

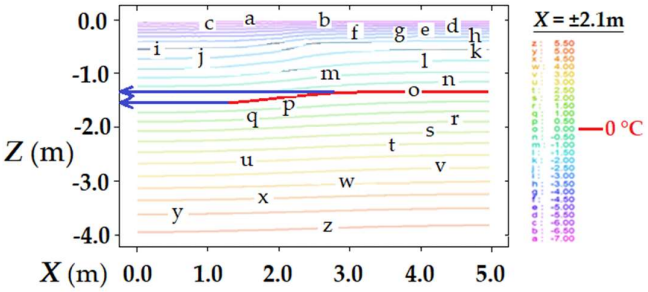


Figure 7. Experiments after the IC4 for X = ±2.10 m—evaluation of freezing depth.

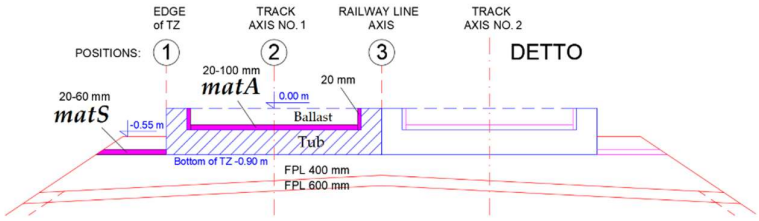


Figure 8. Optimal design of the solution against freezing of the TZ structures.

In warmer weather of the pre-periods IC1 and IC2 at the time before the modeling of the experiment, the construction of the transition structure is suitable for frost protection. However, the following IC3 weather values in the previous period are typical for the northern part of Slovakia, where a reinforced concrete tub with a rail bed is partially suitable (Figure 6b, Y = 4.00 m). The freezing depth is less than $h \leq -0.95$ m in the track axis but is no longer suitable for the outer rail (of double track). Therefore, it is not suitable for the outer rail because the frost penetrates from the side slope of the embankment. The above results indicate that the structure is partially freezing here. In this part, sub-ballast mats in thicknesses of 20 to 60 mm can be used (between the reinforced concrete tub and the trackbed in this tub), which will reduce the total freezing depth by 0.04–0.10 m, according to Lai [15] (depending on the used material). The sub-ballast mat is designed to reduce the dynamic effects, according to Wang et al. [14], Hu et al. [20], Hodas and Pultznerova [21], and Shan et. al. [22], but it will also help as a thermal insulation material (in research at DRE in VEGA [18]). In the iron-concrete threshold shown in Figure 6a, frost does not matter but affects the structural layers under this block, the material structure of which may be disturbed.

The weather of pre-period IC4 (Figures 6 and 7) is extremely cold and is unsatisfactory; thus, it will be necessary to use another set of structural layers of the transition zone, for example, various materials with lower thermal conductivity value or with newly added proposed layers under the structure block of the transition zone (bulk or solid) or greater layer thicknesses.

Winter in numerical modeling is the same with a frost index $I_F = -600$ °C·days for all these transition zones models, but the temperature pre-periods IC1 to IC4 are different before it. The layer under consideration had a minor snow cover height $h_{snow} = 0.10$ m, as this ensured an increase in the depth of the freezing of particular layers (because snow is an excellent insulator). In previous research tasks on real in situ models by Hodas et al. [9] and Hodas and Pultznerova [21], the thickness of the snow layer was maintained manually, but for the calculation, it was reduced such that the model was loaded more by frost. Winter without snow or a minor snow layer can occur as well, or the snow layer is modified by the passing of trains.

The final results are shown in Figure 7, which represents a gradual increase in the depth of freezing depending on the weather temperature. These graphs show the freezing of the structural layers of the transition structure element of a double-track railway in a part of its material changes, i.e., reinforced concrete block (position 0–2 m in the calculation) and reinforced concrete tub with a trackbed (2–5 m) under the outer rail (parts under the wheels of the rolling stock).

7. New Optimized "TZ" Frost Protection Design

The research was carried out for different values of the frost index according to the previous considerations, but the final design for the protection of structural layers of TZ against frost is for the coldest periods when undesired freezing of the lower layers occurs. This is especially evident in extreme conditions in frosty winter with a frost index of $I_F = -600$ °C·day and the cold period before winter (IC4).

7.1. Frost Protection of the Construction

In railway practice, the layers under the reinforced concrete tub of the transition zone are not protected (transition between the trackbed track and the fixed track). The biggest problem here is the frost penetrating from the side of the railway body below the transition zone object in position 1 in Figure 8.

The course of frost penetration into layers was investigated in the following positions of the railway object in Figure 8: 1—edge of the transition zone, 2—axis of track No. 1 (detto No. 2), 3—axis of the railway line (model of a double-track railway line). There are various types of materials produced on the market that can be used to protect structural layers, such as various gravel mats, anti-vibration, anti-noise materials, etc. However, it is also necessary to examine their hot air characteristics, as the materials have different coefficients of thermal conductivity λ (W/mK). The lower the coefficient conductivity λ, the better the thermal frost protection. Companies produce these materials for use for various track speeds, for example up to $V = 160$, $V \leq 200$, $V > 200$ km/h, and so on, they state the characteristics of these materials to eliminate static and dynamic effects from train running (vibration, noise, shock, etc.) and with the coefficient of thermal conductivity.

However, there is a missing research area that should deal with the thermal conductivity of materials (not only these materials but all structural layers), i.e., their resistance to the transition of frost through these structural layers. In some cases, they are placed in a reinforced concrete tub (in the case of material as *matA* in Figure 8), but the edge of the transition area in position 1 remains prone to frost. Reinforced concrete has a high coefficient of thermal conductivity (also some other structural layers), and frost penetrates from the side of the TZ structure and the slope of the railway body as well. These structural layers are damaged by frost and maintenance, reconstruction, or eventual new building of the entire transition zone, which is subsequently required (demanding reinforced concrete structure for maintenance during operation).

This paper mainly presents the use of materials in two parts marked as "*matA*" (bath of TZ in concrete ballast tub) and "*matS*" (edge of TZ—the location on the slope of railway body), or we can consider increasing the thickness of the frost protective layer (FPL 400 to 600 mm in Figure 8).

7.2. Design of Materials with Low Coefficient of Thermal Conductivity

The research shows that the best frost protection in positions 1, 2, and 3 of the TZ structure is the material with λ = 0.06 W/m·K, the results of which are in Table 5. The research was carried out for different thicknesses of materials with values λ = 0.06, 0.08, 0.10, and 0.12 W/m·K. Testing was performed on numerical models in SV-HEAT [7], while material thicknesses of 0, 20, 40, 60, 80, and 100 mm were evaluated as under ballast material for *matA* (in concrete ballast tub of the TZ). The sidewalls of the reinforced concrete bathtub of the TZ were lined with the same material *matA*, in all cases, uniformly 20 mm.

Table 5. Depths of freezing—*matA* + *matS* materials: λ = 0.06 W/m·K, thickness 0 to 100 mm.

Position and Material	**Depths of Freezing (m)**					
***MatA* Thickness (mm)**	**0**	**20**	**40**	**60**	**80**	**100**
1—edge of TZ	−1.96	−1.92	−1.88	−1.84	−1.82	−1.81
2—track axis	−1.24	−1.02	−0.81	−0.62	−0.46	−0.42
3—railway line axis	−1.18	−1.01	−0.91	−0.86	−0.80	−0.76
1—edge of TZ (+*matS* 20 mm)		−1.81	−1.77	−1.73		
2—track axis (+*matS* 20 mm)		−0.98	−0.77	−0.52		
3—railway line axis (+*matS* 20 mm)		−1.01	−0.91	−0.78		
1—edge of TZ (+*matS* 40 mm)		−1.77	−1.73	−1.68		
2—track axis (+*matS* 40 mm)		−0.98	−0.73	−0.53		
3—railway line axis (+*matS* 40 mm)		−1.02	−0.91	−0.83		
1—edge of TZ (+*matS* 60 mm)		−1.73	−1.67	−1.65		
2—track axis (+*matS* 60 mm)		−0.97	−0.73	−0.50		
3—railway line axis (+*matS* 60 mm)		−1.02	−0.89	−0.83		
Bottom of the transition zone (TZ)	−0.90	−0.90	−0.90	−0.90	−0.90	−0.90
FPL 400 mm (edge)	−1.51	−1.51	−1.51	−1.51	−1.51	−1.51
FPL 400 mm (track axis)	−1.40	−1.40	−1.40	−1.40	−1.40	−1.40
FPL 400 mm (railway line axis)	−1.30	−1.30	−1.30	−1.30	−1.30	−1.30

Note: More tables and graphs for λ = 0.08 to 0.12 W/m·K are stored at the authors' workplace.

From all possible combinations, a considerable number of tables and graphs was evaluated with the depths of frost penetration into the structures. The example is given in Table 5 with the resulting values in the graph of Figure 9 for λ = 0.06 W/m·K, the results with the best-achieved values; more for λ = 0.08 to 0.12 W/m·K are stored at the authors' workplace.

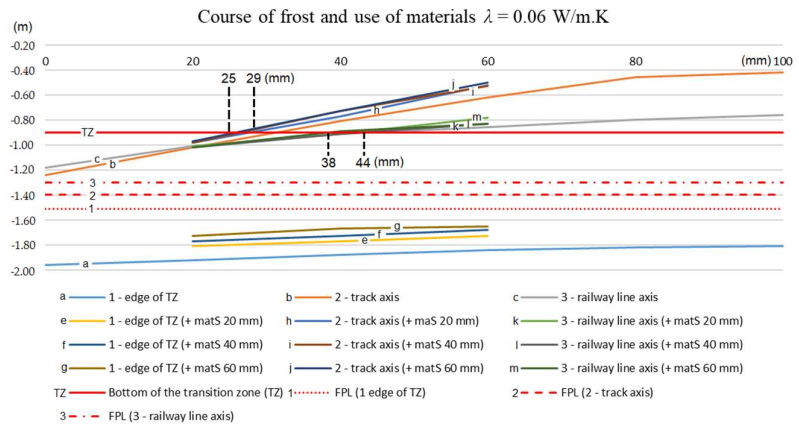


Figure 9. The course of frost and use of materials, λ = 0.06 W/m·K.

According to the research presented in Figure 9 (material with λ = 0.06 W/m·K), the results show that the frost passes through the layers under the reinforced concrete tub of TZ (the bottom surface is at a depth of −0.95 m) in all checked positions: 1, 2 and 3, and in positions 2 and 3, slightly into the protective FPL layer. Position 2: this is for used *matA* for thicknesses from 25 to 29 mm (curves h, I, and j in the track axis), and position 3 is for thicknesses from 38 to 44 mm (curves k, l, and m in the double-track axis). We designed greater material thicknesses than these. The aforementioned values are eliminated by a protective FPL layer with a thickness of 400 mm. However, the research showed that the frost penetration into a considerable depth below the FPL layer in position 1 (edge of TZ) is caused by a lateral entry of frost from the slope.

Similar considerations apply to λ = 0.08 to 0.12 W/m·K, but the frost penetrates deeper (the results for the tables are stored with the authors).

7.3. Optimized Design to Reduce the Effects of Frost

Currently, the basic question is: What measures need to be designed to eliminate the effects of frost penetrating from the side of the transition zone structure? One possibility is to design the incorporation of a material marked *matS* (see Figure 8) with a low coefficient of thermal conductivity λ as already used *matA*. Numerical modeling using SV_HEAT was realized at different thicknesses of the already designed *matA* material, of which we can alternate the thicknesses of the *matS* material. The results of the research showed that the optimal thickness of *matA* was in the range of 20 to 60 mm. The results can be seen in Figure 10 with a detail of the illustration in Figure 11.

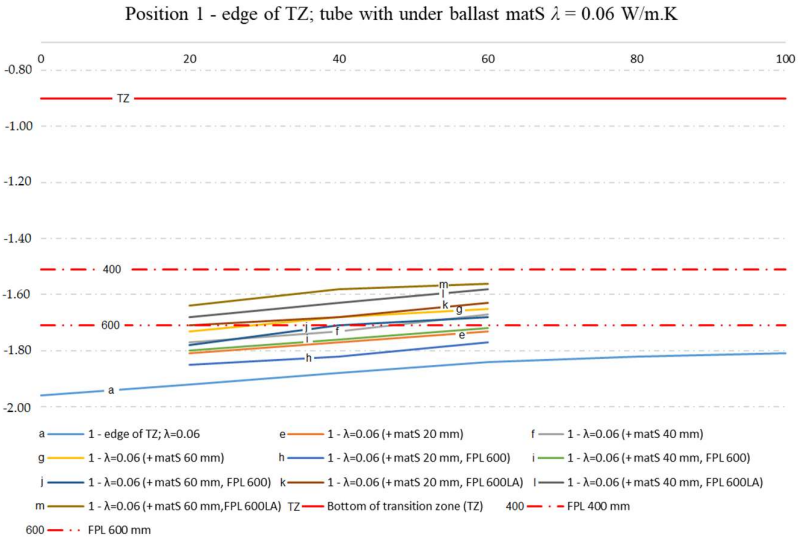


Figure 10. Frost course and used material *matA*: λ = 0.06 W/m·K, *matA* with *matS* 20–60 mm.

The use of the *matS* thermal insulation material in combination with the *matA* reduces the freezing depth but does not eliminate the problem of frost. The next step was to increase the thickness of the frost protective layer (FPL) by the next 200 mm, i.e., to 600 mm in the middle of the railway formation (with a roof cross-slope of 5 %). These measures improve the temperature regime (in winter the passage of frost is eliminated) in the layers in position 1, i.e., edge of the TZ. In positions 2 and 3, it is not necessary to increase the thickness of the protective layer to 600 mm (FPL), but this occurs because the homogeneous continuous layer is easier to build (it is not costly).

The research is valid for cold winters with a frost index of I_F = −600 °C·day (after the IC4 period). For every warmer winter, the structure will work, but the design must be in the coldest winters. It is necessary to emphasize the incorporation of the protection of the transition zones, especially in extreme position 1 of this reinforced concrete structure.

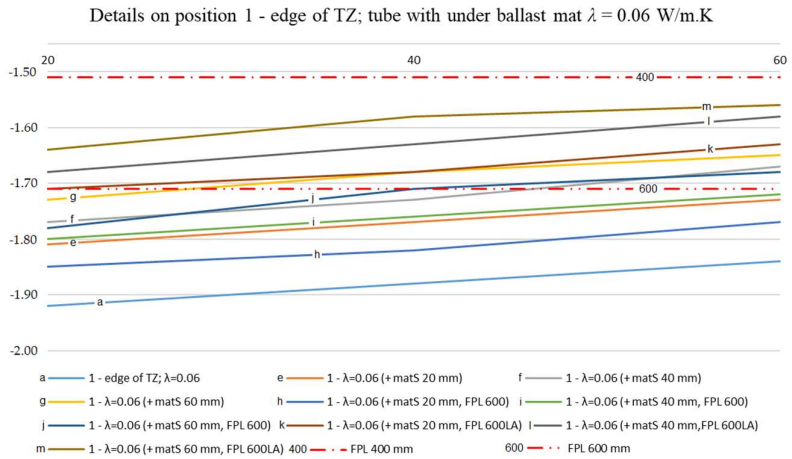


Figure 11. Detail of optimization to eliminate the frost transition through structural layers of TZ with *matA* + *matS*.

8. Conclusions

Creating any 3D model is a challenging task using different types of obstacles while gradually adding its parts. Some models were unsolvable because the SV-HEAT in SVOFFICE [7] did not allow for the calculation. For example, if parts of the model contained inclined surfaces in the longitudinal direction and widened in the transverse direction, then various complicated profiles were created. These models can be created, but the calculations in some parts are unsolvable. For example, if the concrete tub is at a longitudinal slope, then all the layers below this transition part are also at this slope, but the lower and upper edges would go down at the same slope in accordance with the embankment, and this layer would widen. Modeling of this design is possible, but the calculation is not. Therefore, in our experiments of this modeling, the transition structure element is divided into several shorter parts, for example, a part of a reinforced concrete slab with a transition to a tub with a trackbed, the middle and end of this reinforced concrete tub.

In the experiments, the dimensions of the model were proposed according to the actual designs of the objects of the transition zones. Previously, for several years, the created models of single-track and double-track were compared with real objects created in the open-space laboratory of the department DRE as in situ by Hodas and Izvolt [3]; Hodas et al. [9]; Izvolt, Dobes and Hodas [13]; Izvolt, Dobes and Navikas [23]; and Fortunato et al. [24]. Therefore, it can be stated that we obtained the correct relevant results through modeling. Therefore, it is no longer necessary to build in situ models but to directly design and analyze them, which will enable designers to see their design with an analysis of the proposed dimensions and materials used concerning the behavior of the object under thermal load in winter.

Based on the research, we can conclude that for frost protection, it is necessary to use construction materials with a low factor λ = 0.06 W/m·K (for commercial reasons we will not name them). From the graphs in Figures 10 and 11, it is clear that sufficient thicknesses of these materials are from 20 to 40 or 60 mm in the middle part of the transition area of the object in positions 2 and 3 of the solved material "*matA*", in Figure 8. To protect the layers in the edge position 1 in the area with "*matS*", where the frost penetrates from the side, it is necessary to add other materials with thicknesses of 20 to 40 mm.

In the case of regions with a high frost index $I_F \leq -600$ °C·day (and IC4) and lower, it is necessary to increase the protective base layer FPL to 600 mm (in Figure 10). We can also spray parts of the transition zones with ballast bonding methods—ballast stones bonding using adhesives.

In the area of TZ, it is necessary to incorporate qualitatively better material (values for example according to Table 1) and prepare further measures, i.e., for example, to reduce the moisture in the layers using good quality drainage and to use clean, uncontaminated material.

The research results (as well as the inputs and numerical modeling) are valid worldwide, as the designs are carried out for the most adverse winter conditions. These bad conditions can occur 2–3 times in a period of 10 years in countries where a classic winter takes place.

Railway companies and consortia have mechanization tools, construction machinery, and developed procedures for the construction of the proposed railway facilities, including transition zones. They are able to build these technologies. An important factor is the quality of the buildings of the railway lines, including the objects that reduce the effects of dynamic forces and frost in the lower structural layers. The transition zone must be of good quality such that during the operation of railway vehicles (high axle wheel pressures, dynamic effects, frost effects, etc.), the spatial position of the track geometry is sustainable. A quality facility requires less maintenance during operation, which reduces costs.

Author Contributions: Conceptualization, S.H. and A.P.; methodology, S.H.; software, S.H. and A.P.; validation, S.H. and J.I.; formal analysis, S.H.; investigation, S.H. and A.P.; resources, S.H. and J.I.; data curation, S.H.; writing—original draft preparation, S.H. and A.P.; writing—review and editing, S.H. and A.P.; visualization, S.H.; supervision, S.H. and A.P.; project administration, S.H.; funding acquisition, S.H. All authors have read and agreed to the published version of the manuscript.

Funding: This research received no external funding.

Institutional Review Board Statement: Not applicable.

Informed Consent Statement: Not applicable.

Data Availability Statement: Not applicable.

Acknowledgments: The presented parts of the paper were created within the framework of the research activities VEGA 1/0084/20 [18] by the Department of Railway Engineering and VEGA 1/0643/21 [19] by the Department of Geodesy at the Faculty of Civil Engineering of the University of Zilina (FCE-UNIZA).

Conflicts of Interest: The authors declare no conflict of interest.

References

1. Wang, H.; Markine, V.; Liu, X. Experimental analysis of railway track settlement in transition zones. *Proc. Inst. Mech. Eng. Part F J. Rail Rapid Transit* **2018**, *232*, 1774–1789. [CrossRef] [PubMed]
2. Dobes, P.; Izvolt, L.; Hodas, S. Examining the influence of railway track routing on the thermal regime of the track substructure—Experimental monitoring. In *Smart and Green Solutions for Transport Systems, Proceedings of the 16th Scientific and Technical Conference Transport Systems. Theory and Practice 2019, Katowice, Poland, 6–18 September 2019*; Springer Nature: Cham, Switzerland, 2020; Volume 1, pp. 201–209. [CrossRef]
3. Hodas, S.; Izvolt, L. Modeling of temperature regime of railway track structure and its comparison with the results of experimental measurements. In Proceedings of the COMPRAIL XIV Railway Engineering Design and Optimization, Rome, Italy, 24–26 June 2014; Brebbia, C.A., Ed.; WESSEX Institute of Technology, WIT Press: Southampton, UK, 2014; Volume 14, pp. 253–265.
4. Hodas, S.; Pultznerova, A. Freezing of the sub-ballast layers of the railway formation—High embankment and double track. *Civ. Environ. Eng. Sci. Tech. J.* **2019**, *1*, 5–12. [CrossRef]
5. Sestakova, J.; Izvolt, L.; Mocova, L. Research of track geometry quality indicators in transition areas of the railway superstructure. In Proceedings of the International Conference on Traffic and Transport Engineering, Belgrade, Serbia, 27–28 September 2018; City Net Scientific Center: Belgrade, Serbia, 2018; pp. 682–690.
6. Coelho, B.Z.; Hicks, M. Numerical analysis of railway transition zones in soft soil. *Proc. Inst. Mech. Eng. Part F J. Rail Rapid Transit* **2016**, *230*, 1601–1613. [CrossRef]
7. SV-HEAT 2D/3D. Finite element—freeze/thaw modeling, FlexPDE. In *SVOFFICE—Geotechnical Modeling Suite; SVOFFICE^{TM}5/GE and SV-HEAT^{TM}GE*; SoilVision Systems Ltd.: Saskatoon, SK, Canada, 2022; Available online: http://www.soilvision.com (accessed on 25 January 2022).
8. KRAB. KZV—Commercial Railway Research. 2021. Available online: https://kzv.cz/video/ (accessed on 25 April 2022).
9. Hodas, S.; Izvolt, L.; Dobes, P. Preliminary results and conclusions from mathematical modeling of thermal regime of railway track structure. *Int. J. Comput. Methods Exp. Meas.* **2016**, *4*, 69–79.
10. Izvolt, L.; Dobes, P.; Hodas, S. Impact of the method of rail track routing on the thermal regime of subgrade structure—Numerical modeling of non-traffic load. *Int. J. Transp. Dev. Integr.* **2018**, *2*, 250–257.

11. Izvolt, L.; Dobes, P.; Pies, J. Verification of boundary conditions of numerical modeling of the track substructure thermal regime—Influence of the snow cover. *Arch. Transp. J. Pol. Acad. Sci. Comm. Transp.* **2018**, *48*, 51–60. Available online: http://www.archivesoftransport.com/eaot/2018/04/004.pdf (accessed on 24 January 2022). [CrossRef]
12. Sestakova, J.; Dobes, P. Influence of frost protective layers on the realization of the track bed structure. In *Theoretical Foundation of Civil Engineering*; IOP Publishing: Zilina, Slovakia, 2019; pp. 1–9. [CrossRef]
13. Izvolt, L.; Dobes, P.; Hodas, S. Experimental monitoring and numerical modeling of the thermal regime of selected track substructures. *Transp. Probl. Int. Sci. J.* **2019**, *14*, 89–100. [CrossRef]
14. Wang, H.; Markine, V. Methodology for the comprehensive analysis of railway transition zones. *Comput. Geotech.* **2018**, *99*, 64–79. [CrossRef]
15. Lai, B.T.; Fabbri, A.; Wang, H.; Branque, B. Poroelastic behavior of fine compacted soils in the unsaturated to saturated transition zone. *Comput. Geotech.* **2016**, *69*, 627–640. [CrossRef]
16. Navikas, D.; Bulevicius, M.; Sivilevicius, H. Determination and evaluation of railway aggregate sub-ballast gradation and other properties variation. *J. Civ. Eng. Manag.* **2016**, *22*, 699–710. [CrossRef]
17. Navikas, D.; Sivilevicius, H. Modeling of snow cover thickness influence on the railway construction temperature regime under variable weather conditions. *Procedia Eng.* **2017**, *187*, 124–134. [CrossRef]
18. VEGA 1/0084/20. Numerical and experimental analysis of transition zones of objects of structures of railway superstructures and objects of formation substructure. In *Scientific Research*; Department of Railway Engineering, Faculty of Civil Engineering, University of Zilina: Zilina, Slovakia, 2022.
19. VEGA 1/0643/21. Analysis of spatial deformations of the railway track focused on terrestrial laser scanning. In *Scientific Research*; Department of Geodesy, Faculty of Civil Engineering, University of Zilina: Zilina, Slovakia, 2022.
20. Hu, P.; Zhang, C.; Wen, S.; Wang, Y. Dynamic responses of high-speed railway transition zone with various subgrade fillings. *Comput. Geotech.* **2019**, *108*, 17–26. [CrossRef]
21. Hodas, S.; Pultznerova, A. Modeling of railway track temperature regime with real heat-technical values for different climatic characteristics. *Civ. Environ. Eng. Sci. Tech. J.* **2017**, *13*, 134–142. [CrossRef]
22. Shan, Y.; Albers, B.; Savidis, S. Influence of different transition zones on the dynamic response of track-subgrade systems. *Comput. Geotech.* **2013**, *48*, 21–28. [CrossRef]
23. Izvol, L.; Dobes, P.; Navikas, D. Comparison of the dimensions design methodologies of the railway trackbed structure according to frost effect in Slovakia and Lithuania. *J. Civ. Eng. Manag. J. Vilnius Gedim. Tech. Univ. Lith. Acad. Sci.* **2019**, *25*, 646–653. Available online: https://journals.vgtu.lt/index.php/JCEM/article/view/10540/8986 (accessed on 15 November 2021).
24. Fortunato, E.; Paixao, A.; Calcada, R. Railway track transition zones: Design, construction, monitoring, and numerical modelling. *Int. J. Railw. Technol.* **2013**, *2*, 33–58. [CrossRef]